Imaging scatterometry and microspectrophotometry of lycaenid butterfly wing scales with perforated multilayers

Wilts, Bodo D.; Leertouwer, Heinrich; Stavenga, Doekele

Published in:
Journal of the Royal Society Interface

DOI:
10.1098/rsif.2008.0299.focus

Publication date:
2009

Interface focus

J. R. Soc. Interface (2009) **6**, S185–S192
doi:10.1098/rsif.2008.0299.focus
Published online 9 September 2008

Imaging scatterometry and microspectrophotometry of lycaenid butterfly wing scales with perforated multilayers

Bodo D. Wilts, Hein L. Leertouwer and Doekele G. Stavenga*

Department of Neurobiophysics, University of Groningen, NL 9747 AG Groningen, The Netherlands

We studied the structural as well as spatial and spectral reflectance characteristics of the wing scales of lycaenid butterfly species, where the scale bodies consist of perforated multilayers. The extent of the spatial scattering profiles was measured with a newly built scatterometer. The width of the reflectance spectra, measured with a microspectrophotometer, decreased with the degree of perforation, in agreement with the calculations based on multilayer theory.

Keywords: structural colour; spatial scattering profile; reflectance spectra; perforation factor

1. INTRODUCTION

Butterflies derive their attractive coloration from the patterning of scales on the wings. The scattering of incident light by the scale structures as well as the wavelength-selective absorption by pigments determines the colour of the scales. The light scattering is usually incoherent when the scale structures are irregularly organized, but the scattering becomes coherent when there are ordered scale elements, thus giving rise to often striking iridescent colours (Mason 1926, 1927; Ghiradella 1989; Nijhout 1991; Vukusic & Sambles 2003). A particularly interesting butterfly family in this respect is the Lycaenidae, where the male wings generally feature bright structural reflections. The subfamily Polyommatinae have thus obtained their common name, the Blues. Also the males of many species belonging to the Theclinae, the Hairstreaks,have blue wings, but other species display green or silvery iridescences. The Lycaeninae, the Coppers, commonly have a reddish pigmentary coloration, but also some males have blue or violet iridescent wings (e.g. the Violet Copper, *Lycaena helle*), or may even display a metallic orange shine (e.g. the Scarce Copper, *Lycaena virgaureae*; Vigneron *et al.* 2005).

Butterfly wing scales are leaf-like, long, flattened sacs of dried cuticle. Their lower lamina side (adwing) is often smooth and has no prominent microstructure, while the upper (abwing) lamina is marked by longitudinal ridges, connected by cross-ribs. The cross-ribs are joined to the lower lamina by trabeculae (Ghiradella 1989, 1998). In the body of the structurally coloured wing scales of Lycaenidae, in between both laminae, elaborate structures exist that cause the iridescence.

*Author for correspondence (d.g.stavenga@rug.nl).

One contribution of 13 to a Theme Supplement 'Iridescence: more than meets the eye'.

Extensive anatomical studies of lycaenid wing scales have revealed three different spatial organizations that give rise to structural colours (Tilley & Eliot 2002). In the first type, the so-called *Morpho*, each ridge is elaborated into lamellae, which together act as a multilayered reflector. In the second type, *Urania*, multilayers exist in the scale body (Mason 1927). These multilayers often have quite prominent perforations, characteristic of the species (Schmidt & Paulus 1970; Ghiradella 1989; Biro *et al.* 2007; Ingram & Parker 2008). In a third scale type, the scale body has more complicated three-dimensional architectures (Morris 1975; Ghiradella 1989; Kertész *et al.* 2006; Biró *et al.* 2007). For the Green Hairstreak, *Callophrys rubi*, the three-dimensional structures have recently been concluded to be gyroids (Michielsen & Stavenga 2008). The different scale structures appear to be modifications or elaborations of simpler structures common to all scales (Ghiradella 1989).

A central question is of course which optical mechanisms determine the scales' spatial and spectral scattering properties, and thus the wing colour. We therefore have performed a combined study, applying scanning electron microscopy (SEM), imaging scatterometry (ISM) and microspectrophotometry (MSP), on a number of lycaenids with scales having perforated multilayers. Calculations using classical multilayer theory suggest that the function of the perforations is to decrease the bandwidth of the reflectance spectra.

2. MATERIAL AND METHODS

2.1. Butterflies

The investigated scales were from lycaenid butterflies obtained from Dr K. Arikawa (Sokendai, Hayama, Japan), Dr M. F. Brady (Palmerston, Australia),

Received 11 July 2008
Accepted 18 August 2008

Table 1. Distances of the wing scale ridges, d_r, and cross-ribs, d_c, and the perforation factor, p, of the investigated lycaenid wing scales.

	d_r (μm)	d_c (μm)	p
Polyommatinae			
Celastrina argiolus	1.8–2.1	0.6–0.9	0.28±0.06
Danis danis	1.8–2.5	0.9–1.8	0.24±0.07
Plebejus icarioides	1.5–1.8	0.8–1.9	0.26±0.01
Polyommatus icarus	1.3–1.7	0.6–0.8	0.35±0.07
Theclinae			
Arhopala amantes	2.2–2.9	0.8–1.7	0.16±0.04
Arhopala japonica	2.1–2.7	0.8–1.7	0.27±0.03
Chrysozephyrus aurorinus	2.3–2.9	0.6–1.3	0.03±0.03
Chrysozephyrus brillantinus	2.4–2.7	0.6–1.4	0.01±0.01
Hypochrysops delicia	1.4–2.0	0.9–2.1	0.01±0.01
Jalmenus evagoras	2.1–2.6	1.0–1.7	0.07±0.05
Ogyris amaryllis	1.8–2.1	1.5–1.8	0.04±0.03

Dr I. Osipov (Jamison, PA), or locally captured. We studied only structurally coloured lycaenids. Mounted specimens of the studied species were photographed in the butterfly collection of Naturalis, the National Museum of Natural History (Leiden, The Netherlands). Of the subfamily Polyommatinae, we investigated *Celastrina argiolus* (Holly Blue), *Danis danis* (Large Green-Banded Blue), *Plebejus icarioides* (Boisduval's Blue) and *Polyommatus icarus* (Common Blue), and of the subfamily Theclinae we studied *Arhopala amantes* (Large Oak Blue), *Arhopala japonica* (Japanese Blue), *Chrysozephyrus aurorinus*, *Chrysozephyrus brillantinus*, *Hypochrysops delicia* (Moonlight Jewel), *Jalmenus evagoras* (Common Imperial Blue) and *Ogyris amaryllis* (Satin Azure) (table 1).

2.2. Scanning electron microscopy (SEM)

The structurally coloured scales were investigated by SEM, using a Philips XL-30S and XL-30 ESEM. The scales were therefore sputtered with palladium (for 4.5 min with 800 V and 200 mTorr) in a Hummer sputterer (Technics, Alexandria, VA). A prominent phenomenon encountered was the 'holeyness' of the lamellae visible in the scale windows. This was quantified by calculating first the average greyness values g_c and g_h of window areas with and without holes, and then counting the number of pixels, N_h, with greyness value below $(g_c+g_h)/2$, of the total pixel number within the window area, N_w. The fraction $p=N_h/N_w$ was called the perforation factor. The values given in table 1 are averages of at least five independent measurements.

2.3. Imaging scatterometry (ISM)

Single scales were prepared by gently pressing the butterfly wings to a microscope glass slide, which resulted in an assembly of isolated scales, electrostatically attached to the glass. Subsequently, a scale was collected from the slide with the tip of a glass micropipette, produced with an electrode puller, to which a layer of glue was administered (see Giraldo *et al.* 2008). The scattering profile of the single scale was then investigated with a newly developed ISM, which was designed as follows (figure 1). A pinhole illuminated by a xenon lamp creates a narrow aperture beam

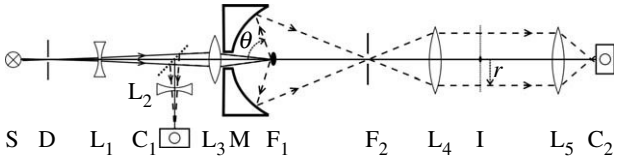

Figure 1. Diagram of the imaging scatterometer. A light source (S) illuminates a pinhole diaphragm (D), which is imaged by lenses L_1 and L_3 on a single butterfly scale, positioned in the first focal point (F_1) of an ellipsoid mirror (M). The scale position is monitored by imaging the scale with lenses L_3 and L_2 on a camera (C_1). The ellipsoid mirror images the scale in the plane of the second focal point (F_2), which coincides with the front focal point of lens L_4. The scale's far-field scattering diagram thus is projected in the back focal plane (I) of lens L_4, which is subsequently imaged by lens L_5 at a second camera (C_2). A spatial filter in plane I, together with a diaphragm in the plane of F_2, suppresses the light transmitted by the scale. The relationship between the scattering angle θ and the distance r in plane I is nonlinear, and therefore the image is corrected for this nonlinearity to obtain a polar scattering diagram.

(approx. 5°), which is focused via an axial hole in an ellipsoid mirror on an object positioned in the first focal point of the ellipsoid. This results in an illumination spot of approximately 10 μm diameter. The light backward scattered by the object is focused in the mirror's second focal point, which coincides with the focal point of a camera objective lens. The far-field radiation pattern of the object thus emerges in the back focal plane of the lens. This plane is subsequently imaged on the photosensitive chip of a digital camera. The obtained image slightly deviates from a polar diagram, because the scattering angle θ is nonlinearly imaged (figure 1); we corrected the final scattering diagram for this nonlinearity. In the scattering experiments with butterfly scales, the scale plane was approximately vertical or about perpendicular to the horizontally directed light beam. The forward scattered, transmitted light appeared to create classical diffraction patterns (Vukusic *et al.* 1999; Kinoshita *et al.* 2008). A spatial filter was therefore placed in the back focal plane of the camera lens, which suppressed the zeroth-order transmitted light; the spatial filter is visible as a black spot in the centre of the scattering

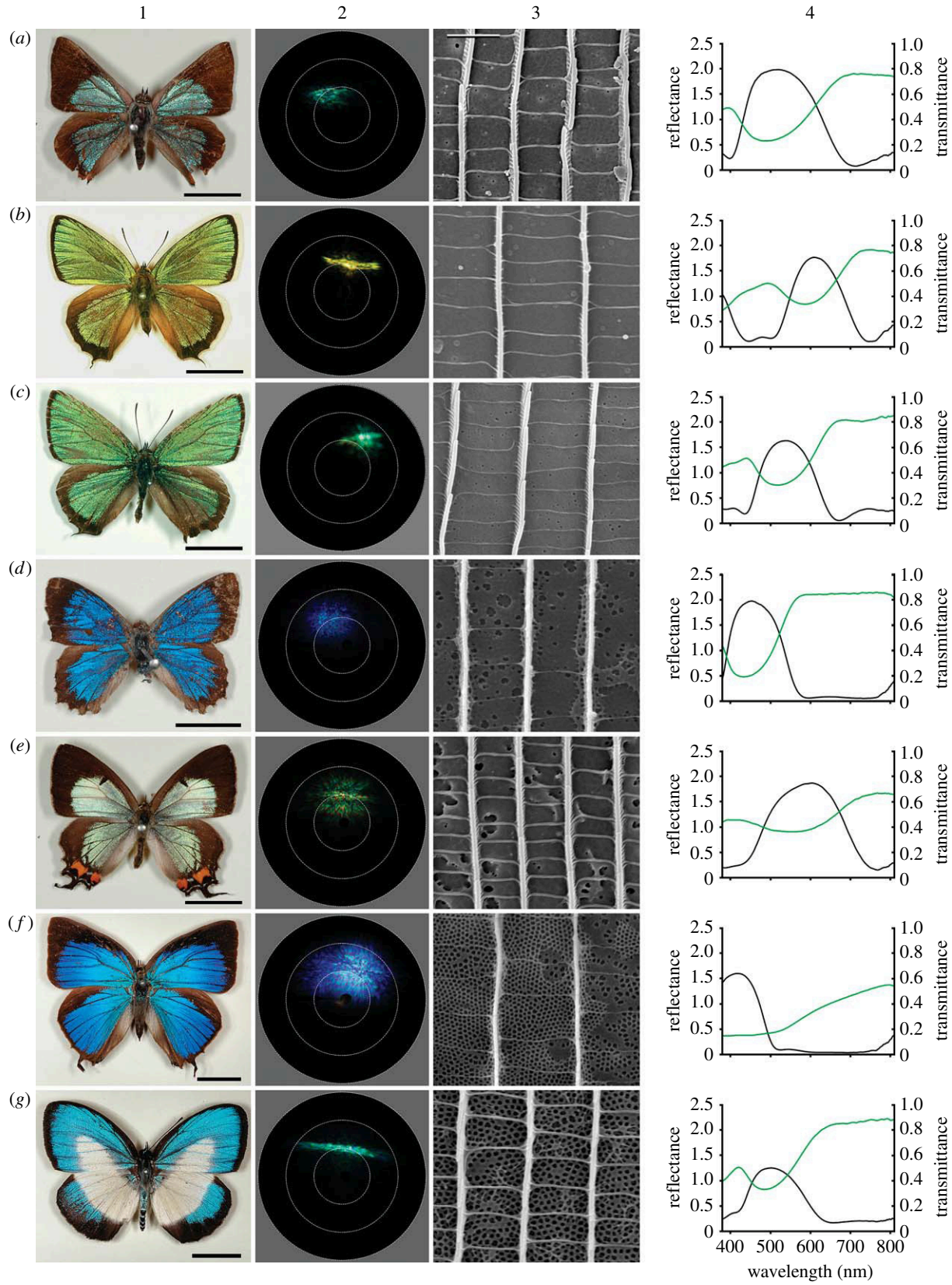

Figure 2. Column 1: photographs of the investigated lycaenid species (scale bars, 1 cm). Column 2: polar diagrams of the backward scattering. The circles indicate angles of 30° and 60°, and the bounding circle represents a 90° scattering angle. The dark line at azimuth 270°, e.g. in (*h*), is the shadow of the horizontally positioned micropipette holding the scale, which is oriented with the longitudinal ridges vertically. The central black spot is due to the spatial filter that blocks the transmitted light. Column 3: scanning electron microscope images of the abwing (upper) side of the scales (scale bar, 2 µm applies to all figures in column 3). Column 4: transmittance (green line) and reflectance (black line) spectra of single scales. The species are ordered according to increasing perforation factor (table 1). (*a*) *Hypochrysops delicia*, (*b*) *Chrysozephyrus brillantinus*, (*c*) *Chrysozephyrus aurorinus*, (*d*) *Ogyris amaryllis*, (*e*) *Jalmenus evagoras*, (*f*) *Arhopala amantes*, (*g*) *Danis danis*, (*h*) *Plebejus icarioides*, (*i*) *Arhopala japonica*, (*j*) *Celastrina argiolus*, (*k*) *Polyommatus icarus*.

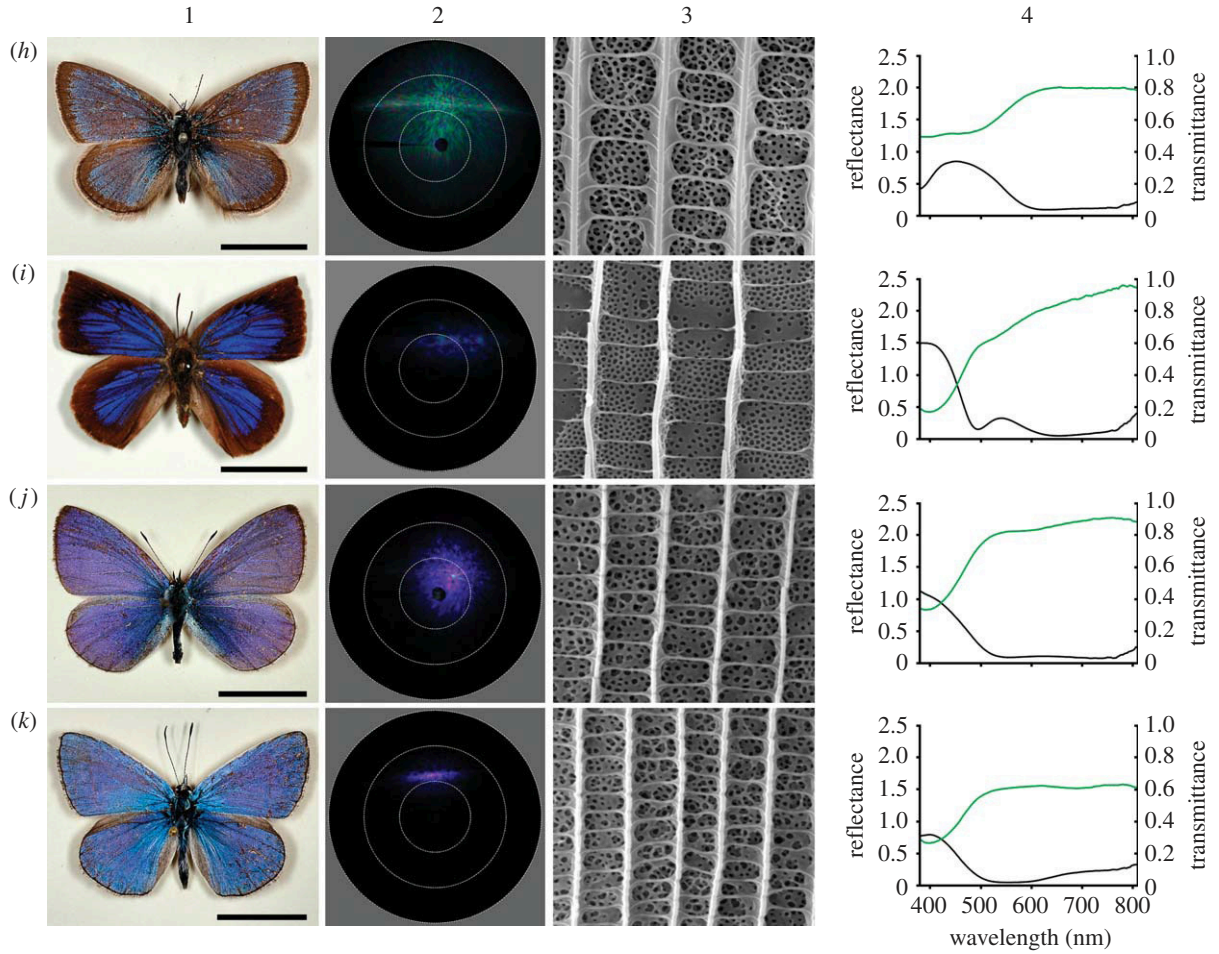

Figure 2. (*Continued.*)

diagrams. A diaphragm in the plane of the second focal point of the mirror blocked the higher orders, so that only light reflected by the scale reached the camera. In the experimental results of figure 2, column 2, the scales were slightly rotated away from the vertical plane so that the centre of the scattering pattern did not coincide with the central black spot of the spatial filter. The angle of rotation was 15–20°, so that the centre of the scattering pattern occurred at 30–40° from the centre of the polar plot.

2.4. Microspectrophotometry (MSP)

Reflectance and transmittance spectra were measured from the isolated, single scales with a microspectrophotometer, which consisted of a xenon light source, a Leitz Ortholux microscope and a fibre optic spectrometer (SD2000, Avantes, Eerbeek, The Netherlands); the microscope objective was an Olympus 20x, NA 0.46 (Stavenga *et al.* 2006). In the reflectance measurements, a white reflectance standard (Spectralon, Labsphere, North Sutton, NH, USA) served as the reference. Using a diffuser as a reference results for some cases in reflectance peak values larger than 1, because the scale reflection is always distinctly directional. We note here that the reflectance spectra obtained by using a mirror instead of a white diffuser are evenly contaminated, because the investigated scales have scattering patterns that are incongruent with both reference objects. In the transmittance experiments, the aperture of the illumination beam was limited to within the objective aperture, and the scale was removed for the reference measurement. The spectra at the short-wavelength side are restricted to 380 nm owing to the low transmittance in the ultraviolet of the optical elements of the microspectrophotometer. Subsequent to the MSP, the scales were prepared for SEM.

3. RESULTS

Column 1 of figure 2 presents photographs of the dorsal (upper side) wings of the studied lycaenids. All wings prominently feature distinct colours, ranging from the violet to green-yellow and silvery-whitish. The hue in most cases changes notably with the angle of observation, and because the colours are hence structurally based, we investigated the structure of the wing scales with SEM.

Column 3 shows SEM photographs of single scales taken from the structurally coloured wing areas. Prominently visible are the (vertically oriented) longitudinal ridges, which are connected by (horizontally oriented) cross-ribs. The distances of the ridges (d_r) and cross-ribs (d_c), determined from both light and scanning electron micrographs, distinctly vary among the species (table 1).

The scale bodies, visible through the windows between the ridges and cross-ribs, are filled with more or less perforated lamellae (figure 2, column 3).

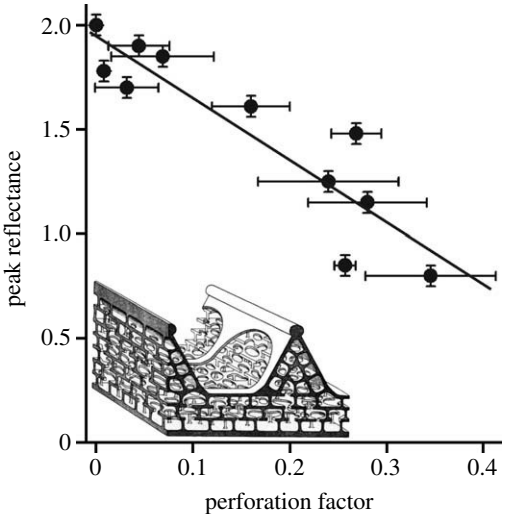

Figure 3. Dependence of the maximum value of the reflectance spectra of figure 2, column 4, on the perforation factor determined from scanning electron microscope photographs such as those in figure 2, column 3. The line is a linear fit. Inset: three-dimensional structure of the scales of the Blues *Plebejus argus* and *Polyommatus coridon* as derived from transmission electron micrographs by Schmidt & Paulus (1970; see their fig. 9).

We quantified the degree of perforation by calculating the perforation factor, p (table 1; see §2.2). The species are ordered in figure 2 according to increasing perforation factor.

We measured the spatial scattering properties of single scales with the imaging scatterometer of figure 1. Column 2 of figure 2 presents the obtained scattering diagrams as polar plots. It appears that, for small perforation factors ($p<0.1$; figure 2*a–e*), the angular extent of the scattered light beam is rather limited, but with an increasing perforation factor the scattering spreads over a larger angle.

We measured the spectral scattering properties with a microspectrophotometer (figure 2, column 4). The aperture of the microscope objective is approximately 24°, and thus the limited aperture imposes restrictions on the microspectrophotometrical measurements of the reflectance spectra, because part of the backward scattered light will escape capture by the objective. Although this fraction remains small for the scales with a directional reflectivity (figure 2*a–d*), it is substantial for the white reference standard, which scatters light diffusely. The amplitude of the reflectance spectra hence is strongly exaggerated for the more or less specular scales; we estimate by a factor of approximately 5.

The peak reflectance is closely related to the perforation factor, as shown in figure 3. Of course, the reflectance of a perforated multilayer is inevitably lower than that of a non-perforated multilayer. Furthermore, with increasing perforation scattering occurs over wider angles, so that an increasing part of the scattered light is not collected by the microspectrophotometer.

The transmittance spectra measured simultaneously with the reflectance spectra (figure 2, column 4) show troughs where the reflectance spectra have a peak, as it should be. However, the reflectance and transmittance spectra are not fully complementary because, first, the scales probably contain some absorbing material and, second, part of the transmitted light is lost outside the objective aperture, namely by diffraction.

4. DISCUSSION

We investigated the structure and optical properties of the wing scales of 11 lycaenids (figure 2). The two *Chrysozephyrus* species, *C. aurorinus* and *C. brillantinus*, of figure 2*b*,*c*, with yellow-green and blue-green wings, respectively, have very similar scale parameters (table 1). If the specimens indeed belong to one and the same species, as stated by Korshunov & Gorbunov (1995), we have studied 10 lycaenid species.

Transmission electron micrographs in the literature show that many lycaenids have scale bodies with multilayers, consisting of alternating chitin and air layers (Lippert & Gentil 1959; Schmidt & Paulus 1970; Tilley & Eliot 2002; Biró *et al.* 2007). We determined the perforation factor as the ratio of the missing area and the total area in the top scale layer. Presumably the perforation factor is similar in the various layers (see the inset of figure 3). The number of layers varies among the lycaenid species studied, from three or four layers (*Eumaeus minyas*: Lippert & Gentil 1959; *Plebejus argus* and *Polyommatus coridon*: Schmidt & Paulus 1970; *Celastrina ladon*: Ghiradella 1989) to six or seven layers (*Favonius jezoensis*: Schmidt & Paulus 1970; *Albulina metallica*: Biró *et al.* 2007).

In order to assess the effect of the perforation on the reflectance, we have applied standard multilayer theory (Macleod 1986; Yeh 2005) to a multilayer consisting of chitin and air layers with thickness values $d_c=0.08$ and $d_a=0.10$ µm, respectively (Schmidt & Paulus 1970; see figure 4*e*, inset). When the chitin layers are not fully transparent, owing to light-absorbing components, they have a complex refractive index. Vukusic *et al.* (1999) determined for *Morpho* scales a value of 1.56 for the real component and between 0.050 and 0.065 for the imaginary component (which means that the absorption coefficient is approx. 1.5 μm^{-1}). A continuous, unperforated layer thus can be assumed to have a refractive index $n_c=1.56–0.06i$. The holes in the perforated chitin layers are small compared with the wavelength of light, and hence the layers have effectively a lowered refractive index: $n_{c,eff}=pn_a+(1-p)n_c$ ($n_a=1$ is the refractive index of air). Slightly more complicated expressions for the effective refractive index exist, but values resulting from these formulae differ only to a very minor extent (Stavenga *et al.* 2006). The medium between the perforated chitin layers is actually not pure air, owing to small, connecting pillars with an average distance of 0.2 µm (Schmidt & Paulus 1970), but their contribution to the refractive index will be minor, and so the refractive index of the intermediate layers can be taken to be equal to 1.

Figure 4 presents the reflectance, transmittance and absorptance spectra following multilayer theory for the multilayers consisting of air layers in between three perforated chitin layers, with perforation factors 0, 0.2 and 0.4, respectively, assuming a normally incident

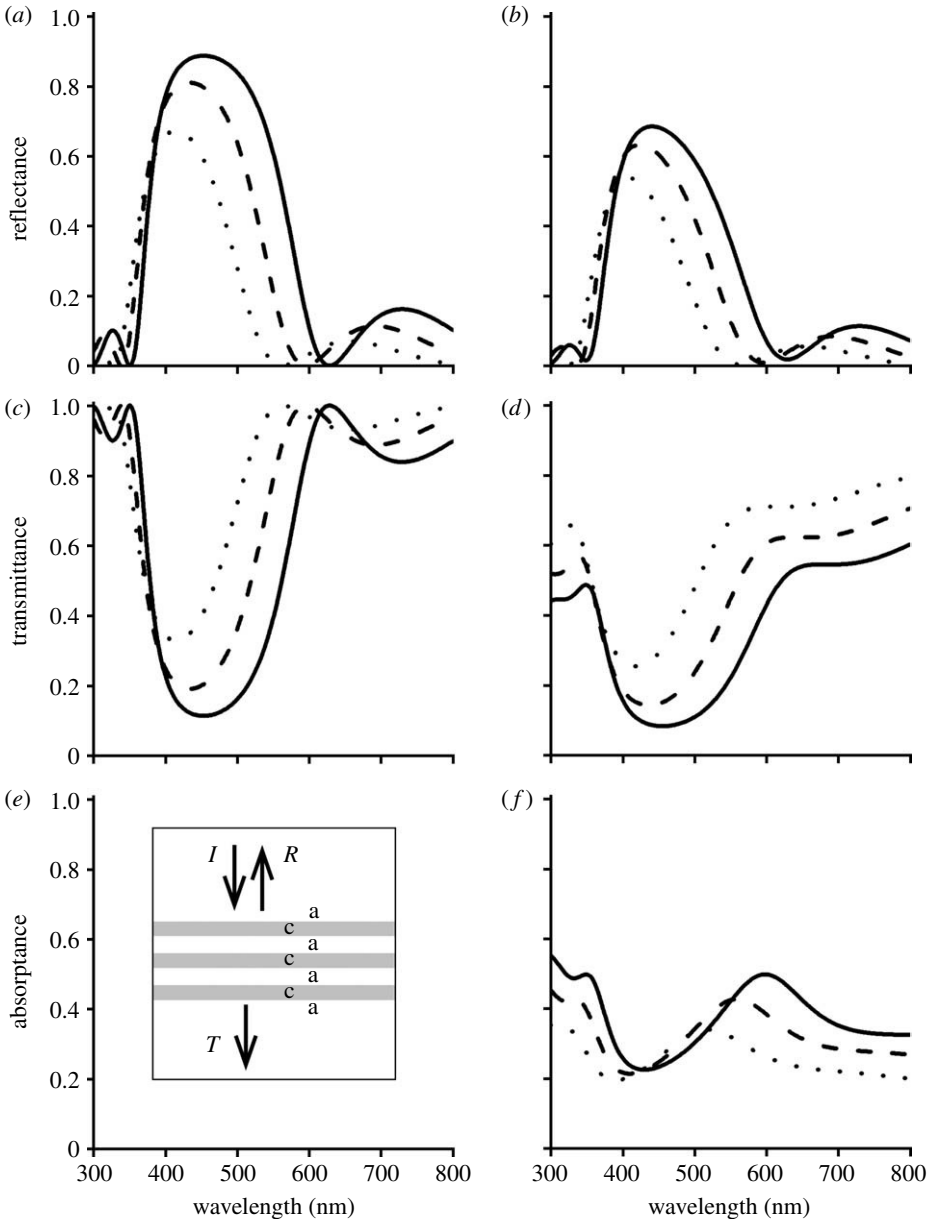

Figure 4. (*a*, *b*) Reflectance (*R*), (*c*, *d*) transmittance (*T*) and (*e*, *f*) absorptance of a lycaenid scale modelled as a multilayer with three perforated layers of chitin, with perforation factor *p* and two intermittent layers of air; a normally incident light flux, *I*, is assumed. The thickness of the chitin and layers (c and a in the inset of (*e*)) is 80 and 100 nm, respectively. The chitin is transparent (real refractive index $n_c=1.56$) in (*a*), (*c*) and (*e*) and it absorbs (complex refractive index $n_c=1.56$–0.06i) in (*b*), (*d*) and (*f*). (*a*–*d*), (*f*) Solid line, $p=0$; dashed line, $p=0.2$; dotted line, $p=0.4$.

light beam. The peak reflectance decreases when the perforation increases as well as when the chitin layers absorb part of the incident light (figure 4*a*,*b*). Furthermore, the width of the reflectance band substantially narrows, from approximately 200 nm for an unperforated multilayer ($p=0$) to approximately 100 nm when the perforation factor becomes $p=0.4$ (cf. Kinoshita *et al.* 2008). Of course, the absorptance is zero when the imaginary part of the refractive index, *k*, is zero (figure 4*e*), but the absorptance is substantial when $k=0.06$ (figure 4*f*).

Figure 5 presents the reflectance spectra for different numbers of layers. For low values of *m*, the number of layers with a high refractive index, the reflectance spectra consist of an asymmetrical central band with lower side bands. When *m* increases to above 5, the central band becomes less asymmetrical and, for unperforated multilayers without absorption ($k=p=0$), approaches a top hat (figure 5*a*; cf. figure 4*c* in the classical paper of Land 1972; note: in that paper *p* is the number of high refractive index layers). For perforated chitin plates, with $p=0.4$, the effective refractive index drops from 1.56 to 1.34. The result is that the central band of the reflectance spectrum of the various multilayers reduces in both height and width (figure 5*b*), but the position of the reflectance peak hardly changes (Land 1972; Kinoshita *et al.* 2008). Taking absorption into account ($k=0.06$; figure 5*c*,*d*) results in reflectance spectra that are overall lower than those of the absorptionless cases; the asymmetry in the central reflectance band for low *m*-values persists with increasing *m*. The effect of absorption on the bandwidth appears to be minor (figure 5*c*,*d* compared with figure 5*a*,*b*, respectively).

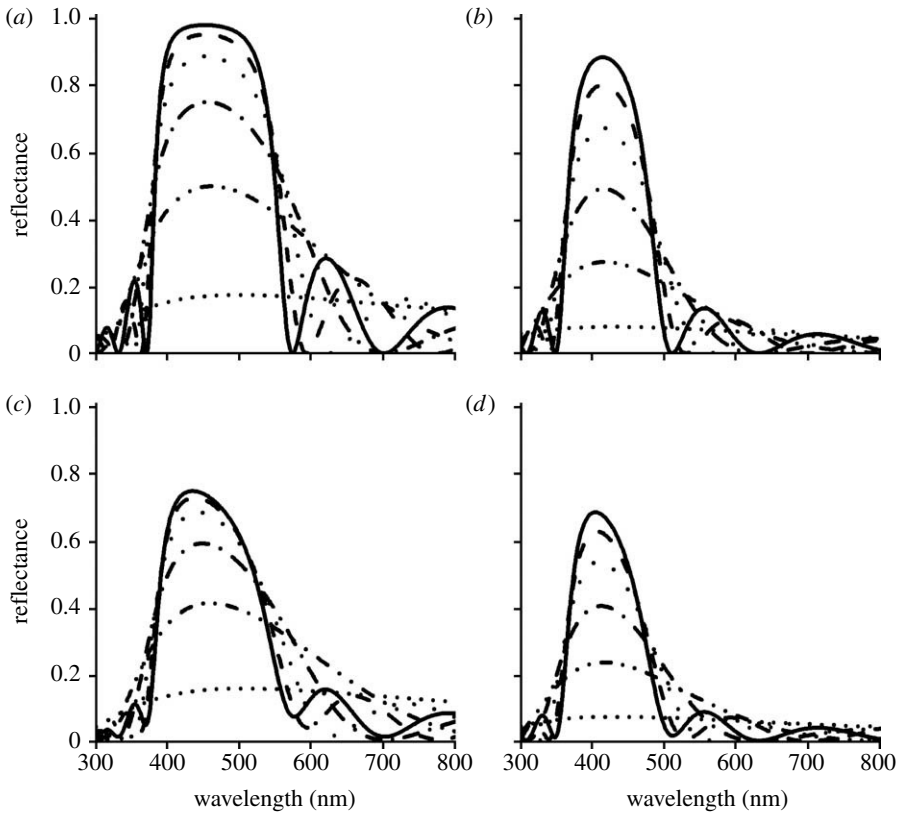

Figure 5. Reflectance spectra calculated for lycaenid scales with a number of m chitin layers (dotted line, $m=1$; double dot-dashed line, $m=2$; single dot-dashed line, $m=3$; dashed line, $m=4$; long-dashed line, $m=5$; solid line, $m=6$) that exhibit no or substantially light absorption ((*a*,*b*) $k=0.0$ and (*c*,*d*) 0.06, respectively) and that are not or substantially perforated ((*a*,*c*) $p=0$ and (*b*,*d*) 0.4, respectively). The values of the layer thicknesses as well as the real part of the chitin refractive index were the same as those in figure 4.

The thickness values of the chitin and air layers of our computational examples approximate the values of the perforated scales of the polyommatine *Albulina metallica* (Biró *et al.* 2007); slightly smaller values are given for various Blues by Schmidt & Paulus (1970); see also Ghiradella (1989). The reflectance peaks following the latter values are shifted towards shorter wavelengths. The comparison of the computed transmittance spectra of figure 4*c*,*d* with the experimental transmittance spectra (figure 2, column 4) suggests that the scales all exhibit absorption, but that their k-value may be somewhat smaller than $k=0.06$, the value used in figures 4 and 5. Further calculations of the spectra based on the actual values of the scale structures of specific species have to await the collection of the necessary data with transmission electron microscopy.

We conclude that a multilayer treatment of the perforated lycaenid scales can provide reasonable insight into their reflectance spectra. However, the applied model assumes that the layers are ideal and extended into infinity, and the reflected beam should thus have the same angular spread as the incident beam, as occurs with a mirror. The experimentally observed scattering diagrams show a much wider spatial spread, however. Inhomogeneities in the scales, as there are the ridges, the irregular perforations and the pillar-like connecting structures between the layers, will be the origin of the spread. The scattering diagrams (figure 2, column 2) often have a broader extent in the horizontal than in the vertical direction. This phenomenon is reminiscent of the extreme, line-shaped scattering pattern of *Morpho* scales, created by the scattering ridges (Vukusic *et al.* 1999; Giraldo *et al.* 2008; Kinoshita *et al.* 2008). To illustrate this, figure 6*a* presents an epi-illumination light-microscopical photograph of a *Chrysozephyrus*

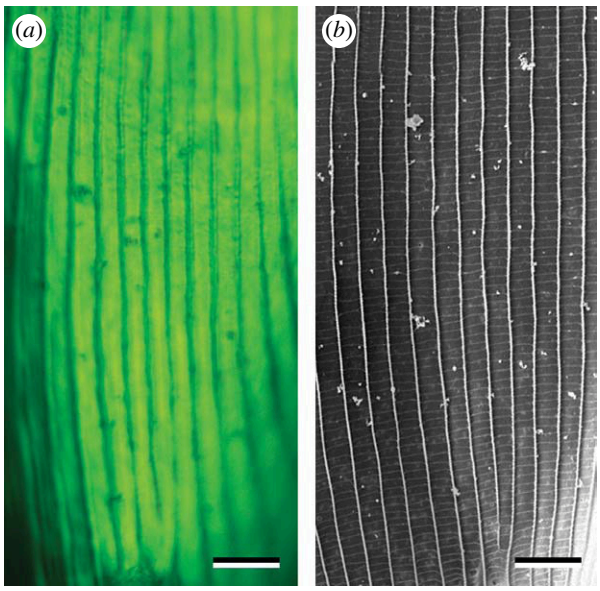

Figure 6. (*a*) Light and (*b*) scanning electron microscope photographs of a scale of *Chrysozephyrus brillantinus*. Scale bars, 10 µm.

brillantinus scale, where the ridges stand out clearly. (The cross-ribs, easily visible in the SEM photograph of the same scale (figure 6*b*), are indiscriminable.) We assume that the longitudinally running scale ridges, directed vertically in the scatterometer experiments of figure 2*b*, column 2, cause the enhanced scattering about the horizontal plane, perpendicular to the ridges.

The scattering diagrams appear not to have a simple relationship with the perforation factor, presumably because several scale properties contribute to the scattering. For instance, the perforation factors of the scales in figure 2*h–j* are almost identical (table 1), but the scattering diagrams differ. Notably figure 2*h*, column 3, shows prominent ridges, which will have caused the horizontal spread of the corresponding scattering diagram. Furthermore, although the perforations in figure 2*i* are more numerous, they are distinctly smaller than those in figure 2*j*, which will result in different scattering diagrams. We conclude therefore that a more complete description of the scattering diagram will necessitate an elaborate three-dimensional photonic crystal theoretical approach. First, however, we need more accurate anatomical data and realistic values of the absorption coefficients. Also, the spectral data obtained by MSP have to be replaced by angle-dependent spectra. Measurements with our imaging scatterometer (figure 1) to achieve that goal are underway.

As a final insight we would like to add that lycaenids apparently can tune their coloration by subtle changes in their scale structures. The reflectance amplitude increases with the number of scale layers; the reflectance peak wavelength can be shifted by slight changes in the thickness and distance of the layers in the scale interior; the bandwidth of the wing reflectance spectrum can be set with the refractive index contrast, i.e. the spectral bandwidth narrows with an increase in perforation; and the spatial extent of the reflected light depends on the detailed sculpting of the scale, whether the perforations are small or large and regular or irregular, and whether the ridges dominate above the scale layers or not. A more extensive comparative survey could elucidate the existence of evolutionary trends.

We thank Dr H. Ghiradella, Dr N. Morehouse, Dr P. Vukusic, Dr S. Yoshioka and Dr M. F. Wehling for critical reading of the manuscript, and M. A. Giraldo for collaboration. Two anonymous referees suggested a number of valuable improvements. B.D.W. obtained an Erasmus Stipendium from the University of Göttingen. This research was supported by AFOSR/EOARD grant no. FA8655-08-1-3012.

REFERENCES

Biró, L. P., Kertész, K., Vértesy, Z., Márk, G. I., Bálint, Z., Lousse, V. & Vigneron, J.-P. 2007 Living photonic crystals: butterfly scales—nanostructure and optical properties. *Mater. Sci. Eng. C* **27**, 941–946. (doi:10.1016/j.msec.2006.09.043)

Ghiradella, H. 1989 Structure and development of iridescent butterfly scales: lattices and laminae. *J. Morphol.* **202**, 69–88. (doi:10.1002/jmor.1052020106)

Ghiradella, H. 1998 Hairs, bristles, and scales. In *Microscopic anatomy of invertebrates* (ed. M. Locke). Insecta, vol. 11A, pp. 257–287. New York, NY: Wiley-Liss.

Giraldo, M. A., Yoshioka, S. & Stavenga, D. G. 2008 Far field scattering pattern of differently structured butterfly scales. *J. Comp. Physiol. A* **194**, 201–207. (doi:10.1007/s00359-007-0297-8)

Ingram, A. L. & Parker, A. R. 2008 A review of the diversity and evolution of photonic structures in butterflies, incorporating the work of John Huxley (The Natural History Museum, London from 1961 to 1990). *Phil. Trans. R. Soc. B* **363**, 2465–2480. (doi:10.1098/rstb.2007.2258)

Kertész, K., Bálint, Z., Vértesy, Z., Márk, G. I., Lousse, V., Vigneron, J.-P., Rassart, M. & Biró, L. P. 2006 Gleaming and dull surface textures from photonic-crystal-type nanostructures in the butterfly *Cyanophrys remus*. *Phys. Rev. E* **74**, 021 922. (doi:10.1103/PhysRevE.74.021922)

Kinoshita, S., Yoshioka, S. & Miyazaki, J. 2008 Physics of structural colors. *Rep. Prog. Phys.* **71**, 076 401. (doi:10.1088/0034-4885/71/7/076401)

Korshunov, Y. & Gorbunov, P. 1995 Butterflies of the Asian Russia (transl. http://pisum.bionet.nsc.ru/kosterin/korgor/lycaen1.htm). Ekaterinburg, Russian Federation: Ural State University Press.

Land, M. F. 1972 The physics and biology of animal reflectors. *Progr. Biophys.* **24**, 77–105. (doi:10.1016/0079-6107(72)90004-1)

Lippert, W. & Gentil, K. 1959 Über lamellare Feinstrukturen bei den Schillerschuppen der Schmetterlinge vom *Urania*- und *Morpho*-Typ. *Z. Morph. Ökol. Tiere* **48**, 115–122. (doi:10.1007/BF00407836)

Macleod, H. A. 1986 *Thin-film optical filters*. Bristol, UK: Adam Hilger.

Mason, C. W. 1926 Structural colors in insects. 1. *J. Phys. Chem.* **30**, 383–395. (doi:10.1021/j150261a009)

Mason, C. W. 1927 Structural colors in insects. 2. *J. Phys. Chem.* **31**, 321–354. (doi:10.1021/j150273a001)

Michielsen, K. & Stavenga, D. G. 2008 Gyroid cuticular structures in butterfly wing scales: biological photonic crystals. *J. R. Soc. Interface* **5**, 85–94. (doi:10.1098/rsif.2007.1065)

Morris, R. B. 1975 Iridescence from diffraction structures in the wing scales of *Callophrys rubi*, the Green Hairstreak. *J. Entomol.* (*A*) **49**, 149–154.

Nijhout, H. F. 1991 *The development and evolution of butterfly wing patterns*. Washington, DC: Smithsonian Institution Press.

Schmidt, K. & Paulus, H. 1970 Die Feinstruktur der Flügelschuppen einiger Lycaeniden (Insecta Lepidoptera). *Z. Morph. Tiere* **66**, 224–241. (doi:10.1007/BF00280735)

Stavenga, D. G., Giraldo, M. A. & Hoenders, B. J. 2006 Reflectance and transmittance of light scattering scales stacked on the wings of pierid butterflies. *Opt. Express* **14**, 4880–4890. (doi:10.1364/OE.14.004880)

Tilley, R. J. D. & Eliot, J. N. 2002 Scale microstructure and its phylogenetic implications in lycaenid butterflies (Lepidoptera, Lycaenidae). *Trans. Lepid. Soc. Jpn* **53**, 153–180.

Vigneron, J. P., Lousse, V., Biró, L. P., Vértesy, Z. & Bálint, Z. 2005 Reflectance of topologically disordered photonic-crystal films. In *Photonic crystal materials and devices III*, vol. 5733 (eds A. Adibi, S.-Y. Lin & A. Scherer). Proc. SPIE, pp. 308–315. Bellingham, WA: SPIE.

Vukusic, P. & Sambles, J. R. 2003 Photonic structures in biology. *Nature* **424**, 852–855. (doi:10.1038/nature01941)

Vukusic, P., Sambles, J. R., Lawrence, C. R. & Wootton, R. J. 1999 Quantified interference and diffraction in single *Morpho* butterfly scales. *Proc. R. Soc. B* **266**, 1403–1411. (doi:10.1098/rspb.1999.0794)

Yeh, P. 2005 *Optical waves in layered media*. Hoboken, NJ: Wiley-Interscience.